Available online at www.sciencedirect.com

Journal of Magnetism and Magnetic Materials 281 (2004) 11–16

www.elsevier.com/locate/jmmm

Surface spin pinning effect of polymer decomposition residues in $CoCr_2O_4$ nanocrystallites system

Shandong Li[a,]*, Hong Bi[b], Zongjun Tian[c], Feng Xu[a], Benxi Gu[a], Mu Lu[a], Youwei Du[a]

[a] *National Laboratory of Solid State Microstructure, Department of Physics, Nanjing University, Hankou Road 22, Nanjing 210093, China*

[b] *College of Chemistry and Chemical Engineering, Anhui University, Hefei 230039, China*

[c] *College of Mechanical and Electronical Engineering, Nanjing University of Aeronautics and Astronautics, Nanjing 210016, China*

Received 31 January 2004; received in revised form 7 March 2004

Available online 20 April 2004

Abstract

$CoCr_2O_4$ nanocrystallites with and without covering of residues from the decomposed polymer at the surface have been fabricated, respectively. It has been revealed that the magnetic properties of the nanocrystallites covered with the residues deviate greatly from those of the ones without residues. In comparison with the "naked" $CoCr_2O_4$ nanocrystallites, for the sample with the covering at the surface, the saturation field, coercivity and loop shift are enhanced remarkably. It is believed that the significant differences in magnetic properties are caused by the presence of residues at the surface.

PACS: 75.75+a; 75.30.Et; 75.30.Gw

Keywords: Surface pinning effect; $CoCr_2O_4$ magnetic properties; Nanometer materials

---

1. Introduction

Magnetic properties of nanocrystallites (NCs), especially the surface magnetic structure and properties, are of great current interest, stemming in part from the development of high-density magnetic storage media with nanosized constituent particles or crystallites. Spin-glass-like surface layer, surface spin canting and a large surface magnetic anisotropy, etc. have been found in some ferro- and ferrimagnetic nanocrystallites, such as Fe, Ni, $NiFe_2O_4$, $CoFe_2O_4$, etc. [1–5]. However, the origin of these anomalous magnetic properties is not completely clear up to now. So it is also necessary to broaden the research range for the further understanding of the mechanism. Despite the large amount of work that has been focused on the magnetic properties of the pure nanocrystallites materials, few reports have been on the organic group covered nanocrystallites.

---

*Corresponding author. Tel.: +86-25-83593817; fax: +86-25-83595535.

E-mail address: sdli@ufp.nju.edu.cn (S. Li).

0304-8853/$ - see front matter © 2004 Elsevier B.V. All rights reserved.
doi:10.1016/j.jmmm.2004.03.040

It is well known that cobalt chromite ($CoCr_2O_4$) has been widely used in dyes, catalyst and the substrate for preparation of film [6]. However, few articles have been reported on the magnetic properties of nanoscaled $CoCr_2O_4$ crystallites, especially those of ones covered by the polymer decomposition residues (PDR) at surface. Therefore, in this paper, the magnetic properties and the surface spin pinning effect were studied by comparing two $CoCr_2O_4$ nanocrystallites systems with and without the covering at the surface.

2. Experimental methods

In order to research the surface effect on the magnetic properties, two kinds of $CoCr_2O_4$ nanocrystallites systems have been prepared: one surface is covered by PDR and the other is naked. For convenience, they were referred as A and B, respectively. The preparation procedures for these two samples are as follows: (1) sample A, 2.0 g copolymer of styrene-co-maleic acid anhydride (SMA) was dissolved in 50 ml *N*,*N*-dimethylamide (DMF) at 353 K in a three-neck bottle, then 1.20 g $CoCl_2 \cdot 6H_2O$ and 2.40 g $CrCl_3 \cdot 6H_2O$ was put into it, the solution was kept stirring under 353 K for 2 h, then it was dropped into excessive distilled water, the precipitate was filtered, washed by distilled water for several times. The dry, solid polymer-metal complex was annealed at 593 K for 8 h at vacuum atmosphere, followed by 833 K for 6 h. Finally, the resulted black powder was oxidized in an air oven at 873 K for 4 h. (2) Sample B, 4.8 g $CoCl_2 \cdot 6H_2O$ and 16 g $Cr(NO_3)_3 \cdot 9H_2O$ were dissolved in 200 ml H_2O and mixed evenly under stirring at room temperature, then 6.4 g NaOH was added, and the mixture was kept stirring at 353 K for 6 h, a kind of grey-green precipitate was filtered and washed by distilled water for several times. Finally the resulted grey-green powder product was annealed in an air oven at 573 K for 2 h and subsequently at 773 K for 3 h.

The magnetic properties of the $CoCr_2O_4$ NCs were measured by using vibrating sample magnetometer (VSM) with a maximum field of 8 T from 300 to 4.2 K. The microstructures of the materials were characterized by a transmission electron microscopy (TEM), high resolution transmission electron microscopy (HRTEM) and an X-ray diffractometer (XRD). The surface characteristic of the NCs was analyzed by Fourier transition infrared spectroscopy (FTIR).

3. Results and discussion

Fig. 1 shows the XRD curves for samples A and B. The indexes of $CoCr_2O_4$ facets signed in Fig. 1 reveal that these two samples are all composed of $CoCr_2O_4$ NCs. The grain sizes calculated by Scherrer equation for samples A and B are 10.5 and 11.2 nm, respectively. This result has also confirmed by TEM observation (not shown here). In order to have a detailed insight into the surface structure for these two samples, HRTEM has been performed for samples A and B, shown in Fig. 2. As illustrated in Fig. 2, the grain features for samples A and B are very similar, and the grain sizes are well consistent with the values of XRD and TEM. However, the grain surface for sample A is covered by a thin PDR layer (pointed out by arrows for some places), while that for sample B is shown a clean surface. It should be mentioned here that the PDR only situates at surface of $CoCr_2O_4$ NCs for sample A, and does not exist in grain in form of impurities. Considering XRD, TEM, and HRTEM results as a whole, it is evident that the

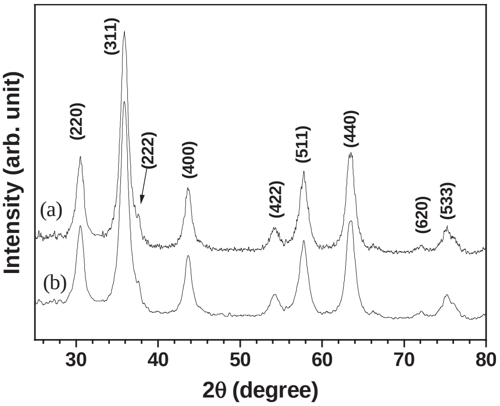

Fig. 1. The XRD traces for samples (a) A and (b) B.

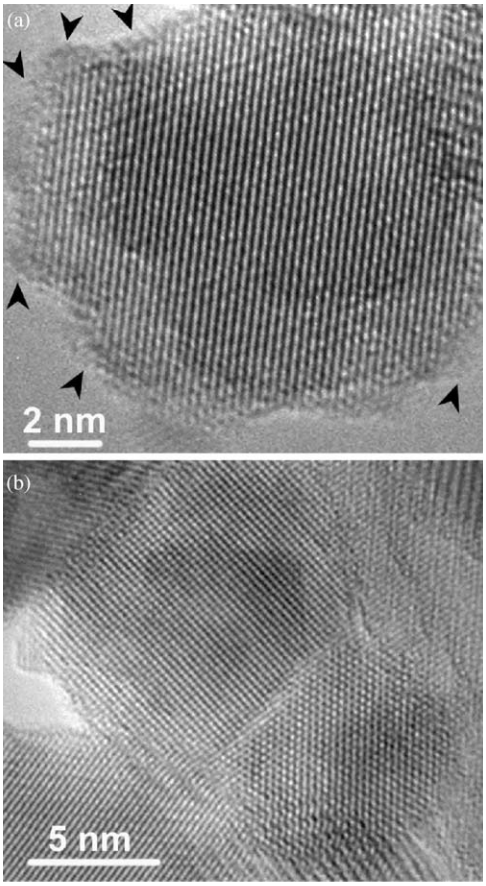

Fig. 2. HRTEM images for samples (a) A and (b) B. The arrows in Fig. 2(a) point out some places covered by PDR layer.

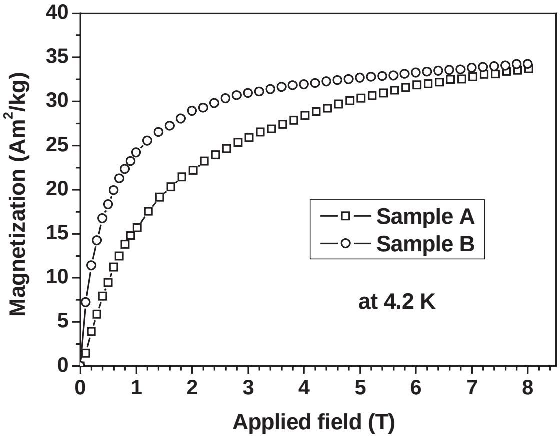

Fig. 3. The initial magnetization curves for samples A and B at 4.2 K.

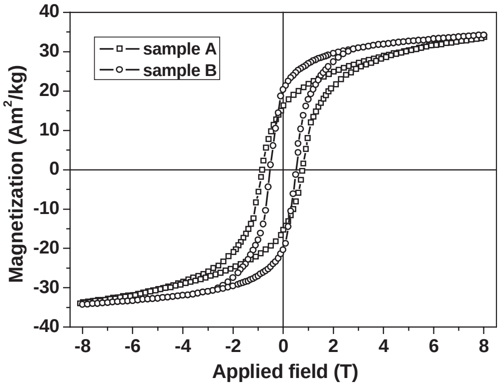

Fig. 4. The hysteresis loops of $CoCr_2O_4$ nanocrystallites for samples A and B at 4.2 K with a cooling field of 8 T.

different magnetic properties described below are attributed to the different surface feature between samples A and B rather than the difference of grain sizes or impurities in sample A.

The magnetic properties at low temperature for these two samples were recorded by a VSM. Shown in Fig. 3 are the initial magnetization curves for samples A and B. As illustrated in Fig. 3, the initial magnetization curve of sample B exhibits a typical ferrimagnetic characteristic. The magnetization of sample B will approach to saturation at high field. However, it is difficult for sample A to reach the saturation state. Even the field rises up to 8 T (the maximum field in the measurement), the magnetization of sample A still increases. This fact suggests that there is a pinning field for sample A which hampers the rotation of magnetic moments to the applied field.

Fig. 4 shows the hysteresis loops of the samples at 4.2 K in the presence of a cooling field of 8 T. As illustrated in Fig. 4a shifted loop of 30.6 kA/m and a very high coercivity of 632.9 kA/m were observed in sample A. While the coercivity for sample B is 416.0 kA/m, which is evidently lower than that of sample A. Moreover, the loop shift was not observed for sample B.

Although samples A and B are all composed of $CoCr_2O_4$ NCs, and have approximately equal grain size, they exhibit significant difference in magnetic properties. In order to study the origin of these differences, besides the observation of HRTEM, the surface characteristic of these two systems was also studied by FTIR and the results are shown in Fig. 5 and Table 1. It can be seen that there is a great difference in the surface characteristic for these two samples. As illustrated in Fig. 5(a), three peaks at 955, 854 and 798 cm^{-1} are assigned to the vibrating of Co(II)–O bond. The peaks at 632 and 523 cm^{-1} originate from the vibrating of Cr(III)–O bond. This result demonstrates the $CoCr_2O_4$ compound in sample A. In addition, there is a large amount of the polymer decomposition residues covering at the surface of $CoCr_2O_4$ NCs. For example, two very strong peaks at 1346 and 1014 cm^{-1} are attributed to an asymmetric and a symmetric vibrating peak of (C–OH), respectively. Two weak shoulder peaks at 1651 and 1429 cm^{-1} locating on the left side of the strong peak at 1346 cm^{-1} are assigned to the vibrating peak of $R_1CH{=}CHR_2$ or $RCH{=}CH_2$. Two small narrow peaks at 749 and 700 cm^{-1} are attributed to the vibrating of C–H of mono-substituted benzyl group. All these residue groups resulted from the decomposition of SMA polymer which containing repeated styrene and maleic acid anhydride units, and absorbed on the surface of $CoCr_2O_4$ NCs during annealing. However, for sample B only Co(II)–O (located at 949, 885, 757 cm^{-1}) and Cr(III)–O (at 624 and 519 cm^{-1}) bonds are observed except for the water peaks at 3421 and 1626 cm^{-1}. The water arises from the absorption of water moisture in air.

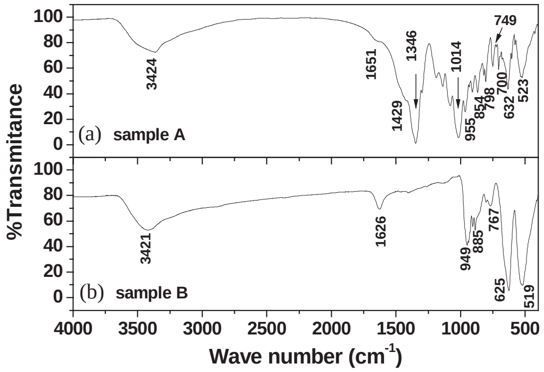

Fig. 5. FTIR spectra for samples (a) A and (b) B.

It is known that bulk $CoCr_2O_4$ has a normal spinel structure, and the magnetic coupling is carried out through the super-exchange interaction between the metal ions via oxygen ions, which is sensitive to the local atomic environment, such as the length and angle of chemical bonds, etc. Variation in coordination of surface cations results in a distribution of net exchange fields. The exchange bonds will be broken if an oxygen ion is missing from the surface. For nanoscaled crystallites, because of the broken symmetry at the surface, broken bonds, and the super-exchange interaction fluctuation in both strength and sign, thus the magnetic structure of the surface corresponds to a spin glass-like configuration or to a spin disordered system [7,8]. For the studied systems, the grain sizes are only about 10 nm, which gives rise to a large ratio of surface area versus volume for a particle. A large amount of ions are located at the surface of the

Table 1
The peak positions and their assignments of FTIR traces for $CoCr_2O_4$ nanocrystallites

Sample	Wavenumber (cm^{-1})	Chemical bond	Origination
A	3424	H–OH	H_2O
	1651, 1429	$R_1CH{=}CHR_2$, $RCH{=}CH_2$	SMA decomposition
	1346, 1014	–C–OH	SMA decomposition
	749, 700	Mono-substituted benzyl	SMA decomposition
	955, 854, 798	Co(II)–O	Oxidation
	632, 523	Cr(III)–O	Oxidation
B	3421, 1626	H–OH	Water moisture
	949, 885, 757	Co(II)–O	Decomposition
	624, 519	Cr(III)–O	Decomposition

nanocrystallites. So the surface layer, to great extent, dominates the magnetic properties.

However, in addition to the size effect and surface effect on the magnetic properties, in the case of these two systems with approximately equal grain size, the significant difference in magnetic properties should be attributed to the different surface magnetic structures caused due to the organic residues at the surface. In fact, the effect of the organic residues at the surfaces on the magnetic properties can be interpreted as the surface pinning effect [9]. The organic residues bonded to the surface lead to the fact that the electrons involved can no longer participate in the superexchange. Accordingly, they will further reduce the effective coordination of the surface cations.

It is well known that the electronic and magnetic configurations of nanocrystallites are dramatically influenced by the chemisorption of polymeric ligand on the surface of nanocrystallites. For example, the ferrite ultrafine crystallites coated by organic molecules, exhibit surface spin canting and a large surface magnetic anisotropy [1,5,9]. Another example is that in nickel carbonyl clusters with CO chemisorption on Ni surface [10], the coordination by CO favors intra-atomic redistribution of the Ni electronic configuration from $3d^{9-x}4s^x$ to $3d^{10}$ (similar to Cu). As a result, the effect of CO ligation is to quench completely the magnetic moments of the surface Ni atoms. The bonding of surfactant molecules is equivalent to a strong ligand field acting on the surface atoms. Such a ligand field causes a very strong pinning of the magnetic moments on metallic ions in the surface layer, which is transferred well into the interior of the crystallite by the magnetic exchange interactions [11,12]. A surface layer with non-collinear spins and a clear separation of core and shell magnetic properties in oxides NCs has been demonstrated by means of Mössbauer spectra and polarized neutron diffraction, etc. [5,12–14]. Therefore, it is reasonable that the surface absorption of the polymer decomposition residues on $CoCr_2O_4$ NCs will act as a kind of ligand pinning, and significantly influence the surface magnetic structure of the $CoCr_2O_4$ NCs. Due to the surface spin pinning effect, the difference of magnetic spin state between the surface layer and the inner core has been enlarged.

The surface spins have multiple configurations for any orientation of the core magnetization [1]. When the sample is cooled in a high magnetic field to a low temperature, the spin canted layer is frozen into a spin-glass-like phase with a minimum total free energy at low temperature for $CoCr_2O_4$ NCs. Furthermore, the spin pinning effect by PDR results in the difficulty to change surface spin configuration from one to another. Therefore, an enhanced coercivity and bias field present are in the PDR-covered sample. In the same way, the difficulty to approach the saturation state for sample A is attributed to this surface spin pinning effect.

4. Conclusion

The enhancement effects of magnetic properties, including a loop shift, coercivity and saturation field, were observed in $CoCr_2O_4$ nanocrystallites with organic residues at the surfaces. These enhancement effects are believed to originate from spin surface pinning effect by the organic residues absorbed at the surfaces of the nanocrystallites.

Acknowledgements

This work is financially supported by National Key Project for Basic Research (G1999064508) and the Nano-technology Laboratory of Jiangsu Province.

References

[1] R.H. Kodama, A.E. Berkowitz, E.J. McNiff, S. Foner Jr., Phys. Rev. Lett. 77 (1996) 394.

[2] T. Ibusuki, S. Kojima, O. Kitakami, Y. Shimada, IEEE Trans. Magn. 37 (2001) 2223.

[3] Z.M. Stadnik, P. Griesbach, G. Dehe, P. Gütlich, T. Kohara, G. Stroink, J. Magn. Magn. Mater. 70 (1987) 439.

[4] A.E. Berkowitz, J.A. Lahut, I.S. Jacobs, L.M. Levinson, D.W. Forester, Phys. Rev. Lett. 34 (1975) 594.

[5] D. Lin, A.C. Nunes, C.F. Majkrzak, A.E. Berkowitz, J. Magn. Magn. Mater. 145 (1995) 343.
[6] G. Hu, Y. Suzuki, Phys. Rev. Lett. 89 (2002) 276601.
[7] A.E. Berkowitz, F.E. Spada, F.T. Parker, in: G.C. Hadajipanayis, R.W. Siegel (Eds.), Nanophase Materials, Academic Press, New York, 1994, p. 587.
[8] A.H. Morrish, K. Haneda, J. Appl. Phys. 52 (1981) 2496.
[9] A.E. Berkowitz, J.A. Lahut, I.S. Jacobs, L.M. Levinson, D.W. Forester, Phys. Rev. Lett. 34 (1975) 594.
[10] D.A. van Leeuwen, J.M. van Tuitenbeek, L.J. de Jongh, A. Ceriotti, G. Pacchioni, O.D. Häberlen, N. Rösch, Phys. Rev. Lett. 73 (1994) 1432.
[11] F. Bødker, S. Mørup, S. Linderoth, Phys. Rev. Lett. 72 (1994) 282.
[12] A.E. Berkowitz, IEEE Trans. Magn. 22 (1986) 466.
[13] R. Pynn, J.B. Hayter, S.W. Charles, Phys. Rev. Lett. 51 (1983) 710.
[14] A.H. Morrish, K. Haneda, J. Magn. Magn. Mater. 35 (1983) 105.